



Iron-rich perovskite in the Earth's lower mantle

Z. Mao ^{a,*}, J.F. Lin ^a, H.P. Scott ^b, H.C. Watson ^c, V.B. Prakapenka ^d, Y. Xiao ^e, P. Chow ^e, C. McCammon ^f

^a Department of Geological Sciences, Jackson School of Geosciences, The University of Texas at Austin, Austin, TX 78712, USA

^b Department of Physics and Astronomy, Indiana University, South Bend, IN 46634, USA

^c Department of Geology and Environmental Geosciences, Northern Illinois University, DeKalb, IL 60115, USA

^d Center for Advanced Radiation Sources, University of Chicago, Chicago, IL 60637, USA

^e HPCAT, Carnegie Institution of Washington, Advanced Photon Source, Argonne National Laboratory, Argonne, IL 60439, USA

^f Bayerisches Geoinstitut, Universität Bayreuth, D-95440 Bayreuth, Germany

ARTICLE INFO

Article history:

Received 14 January 2011

Received in revised form 11 May 2011

Accepted 28 June 2011

Available online 12 August 2011

Editor: L. Stixrude

Keywords:

Fe-bearing perovskite
equation of state
lower mantle
bulk sound velocity
density

ABSTRACT

The equations of state of perovskite with $(\text{Mg}_{0.75}\text{Fe}_{0.25})\text{SiO}_3$ and MgSiO_3 compositions have been investigated by synchrotron X-ray diffraction up to 130 GPa at 300 K in diamond anvil cells. Here we show that the addition of 25% Fe in MgSiO_3 perovskite increases its density and bulk sound velocity (V_Φ) by 4–6% and 6–7%, respectively, at lower-mantle pressures. Based on concurrent synchrotron X-ray emission and Mössbauer spectroscopic studies of the samples, the increase in V_Φ and density can be explained by the occurrence of the low-spin Fe^{3+} and the extremely high-quadrupole component of Fe^{2+} . Combining these experimental results with thermodynamic modeling, our results indicate that iron-rich perovskite can produce an increase in density and a value of V_Φ that is compatible with seismic observations of reduced shear-wave velocity in regions interpreted as dense, stiff piles in the lower mantle. Therefore, the existence of the Fe-rich perovskite in the lower mantle may help elucidate the cause of the lower-mantle large low-shear-velocity provinces (LLSVPs) where enhanced density and V_Φ are seismically observed to anti-correlate with the reduced shear wave velocity.

© 2011 Elsevier B.V. All rights reserved.

1. Introduction

Earth's lower mantle is thought to consist mainly of iron-bearing silicate perovskite and ferropericlase, with a nominal iron (Fe) content of about 10% in perovskite and 20% in ferropericlase (e.g. Hirose, 2002). The addition of Fe in these minerals is known to result in an increase in their densities (e.g. Jacobsen et al., 2002). Of particular importance with respect to seismic observations of the lower mantle are the recently discovered electronic spin-pairing transitions of Fe in ferropericlase and perovskite at lower-mantle conditions (e.g. Badro et al., 2003, 2004; Catalli et al., 2010; Li et al., 2004; Lin et al., 2008; McCammon et al., 2008; Stackhouse et al., 2007; Zhang and Oganov, 2006). The spin transitions of iron have been observed to produce significant changes in density, radiative thermal conductivity and electrical conductivity of lower mantle minerals (e.g. Fei et al., 2007a; Goncharov et al., 2010; Lin et al., 2007; Lin and Tsuchiya, 2008; Ohta et al., 2008). The high-spin (HS) to low-spin (LS) transition of Fe has also been reported to affect the sound velocities of ferropericlase ($(\text{Mg,Fe})\text{O}$), the second most abundant mineral in the lower mantle (Antonangeli et al., 2011; Crowhurst et al., 2008; Marquardt et al., 2009). However, the effect of the spin transitions on

the elasticity of the most abundant perovskite phase remains largely undetermined (e.g. Kiefer et al., 2002).

Previous studies have shown that Fe-bearing perovskite (up to 10–15% Fe) and Fe-free MgSiO_3 perovskite have similar incompressibilities at lower-mantle pressures (e.g. Kiefer et al., 2002; Lundin et al., 2008; McCammon et al., 2008). Due to the differences between the experimental designs of these studies, it is difficult to understand their geophysical implications. Because lower-mantle perovskite is expected to contain 10% iron, studying the elasticity of relatively iron-rich perovskite under controlled experimental conditions is more applicable in evaluating the role of iron-rich regions in the lower mantle. Most importantly, the equation of state (EoS) of Fe-rich perovskite across potential Fe spin transitions has not been investigated at conditions relevant to the lower mantle.

Here, we have conducted high-pressure synchrotron X-ray diffraction (XRD) experiments on perovskite with 25% Fe and without Fe to constrain the effect of Fe on the EoS of perovskite. We have also conducted synchrotron Mössbauer spectroscopy (SMS) to determine the valence states and hyperfine parameters of Fe in perovskite, and synchrotron X-ray emission spectroscopy (XES) measurements that were applied to derive the total 3d spin momentum of Fe. The combined results from XRD, SMS and XES are important to understand the effect of Fe on the elasticity of perovskite in potentially iron-rich regions of the lower mantle, such as large low-shear-velocity provinces (LLSVPs) and ultra-low velocity zones (e.g. Garnero and McNamara, 2008).

* Corresponding author.

E-mail address: zhumao@mail.utexas.edu (Z. Mao).

2. Experimental details

Polycrystalline, ^{57}Fe -enriched enstatite was used as the starting sample for synthesizing perovskite with 25% Fe ($(\text{Mg}_{0.75}\text{Fe}_{0.25})\text{SiO}_3$, Pv25) (Mao et al., 2010). The enstatite sample was examined by X-ray diffraction and electron microprobe to confirm its crystal structure and chemical composition. Based on both conventional and synchrotron Mössbauer spectroscopic analyses, Fe in the synthesized enstatite was mainly in the Fe^{2+} state and its Fe^{3+} content was below the detection limit (Mao et al., 2010). The starting enstatite sample was loaded in a symmetric diamond anvil cell (DAC) and maintained under vacuum before loading with Ne pressure medium in a Re gasket. A Pt foil was placed next to the starting sample to determine the pressure (Fei et al., 2007a). To avoid the formation of ferropericlase and other phases, we directly compressed the sample to 60 GPa at 300 K where we were able to synthesize the single-phase perovskite. The sample was laser heated at 1300 to 1600 K for ~ 2 h to fully transform the starting material to Pv25 at GSECARS of the Advanced Photon Source (APS), Argonne National Laboratory (ANL). The synthesized sample was confirmed by X-ray diffraction to be in the perovskite structure. X-ray diffraction patterns were collected from the samples in 1–3 GPa intervals up to 135 GPa at 300 K. During compression, the synthesized Pv25 was not laser-annealed in order to avoid the decomposition of Pv25. In addition to Pt, X-ray diffraction of Ne was used as a second pressure indicator. The difference in pressure between the Pt and Ne pressure scales used is within ± 2 GPa (Fei et al., 2007b).

Fe-free MgSiO_3 -perovskite was synthesized from MgSiO_3 enstatite glass, which was mixed with Pt. The mixture was also loaded with Ne pressure medium and compressed to 30 GPa at 300 K, and then laser heated between 1500 and 2000 K for ~ 2 h at GSECARS of the APS, ANL. X-ray diffraction patterns of Pv were taken at 1–3 GPa intervals from 30 GPa to 120 GPa, and the sample was laser-annealed every 10 GPa to reduce the potential deviatoric stress.

To determine the electronic states and the hyperfine parameters of Fe in Pv25, SMS measurements of the Pv25 used for the XRD experiments were also conducted at HPCAT of the APS, ANL using an incident X-ray beam with an energy resolution of 2 meV. We collected SMS spectra of the Pv25 sample at 135 GPa and 300 K with or without a ~ 10 μm thick stainless steel foil with a natural ^{57}Fe abundance. The stainless steel foil was placed in front of the sample and used as a reference to determine the chemical shift (CS) of the Fe sites. The collection time for each spectrum was four to five hours.

XES measurements of Pv25 were conducted at HPCAT of the APS, ANL to examine the total spin momentum of Fe. Pv25 was synthesized from the same enstatite sample used for XRD. The starting enstatite was sandwiched between two dried NaCl layers and loaded in a DAC with a pre-indented Be gasket and cBN gasket insert. The incident energy of the X-ray for the XES experiments was set at 11.35 keV with an energy bandwidth of approximately 1 eV. The XES spectra were collected at 80, 95, 119 and 135 GPa. The pressure was determined by the ruby R_1 fluorescence shifts and doubled-checked by the Raman shift of the diamond culet (Akahama and Kawamura, 2006; Mao et al., 1986). The collection time for each XES spectrum was about 40 min, and 35–40 spectra were collected and added together at each given pressure. The reference HS and LS spectra were collected from ferropericlase with 25% Fe at ambient conditions and at 90 GPa and 300 K, respectively (Lin et al., 2010; Mao et al., 2010).

3. Results

The measured diffraction patterns matched the diffraction lines of Pv25 (or Pv), except one belonging to the strongest peak of stishovite (Fig. 1) (O'Neill and Jeanloz, 1994). No signs of ferropericlase was observed in the diffraction patterns. We used 9–13 peaks to calculate the cell parameters for Pv and Pv25. The pressure–volume relations

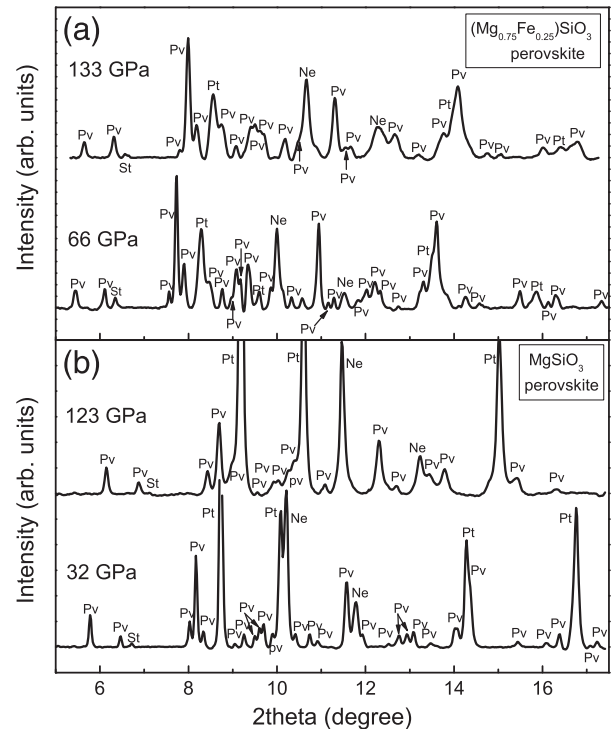


Fig. 1. Representative angle-dispersive X-ray diffraction patterns of perovskite at high pressures. (a) Perovskite with 25% Fe at 66 and 133 GPa. (b) Fe-free perovskite at 32 and 123 GPa. Incident X-ray wavelength, $\lambda = 0.3344$ Å.

show that the density of Pv25 is 4% greater than that of Pv at 130 GPa (corresponding to 2800 km in depth), indicating that the addition of iron can significantly increase the density of perovskite at lower-mantle pressures (Fig. 2). Fitting the pressure–volume data using the third-order Birch–Murnaghan EoS yields $K_0 = 335(\pm 8)$ GPa with $V_0 = 159.3(\pm 0.6)$ Å³ with a fixed $K_0' = 4$ for Pv25, and $K_0 = 259.6(\pm 2.8)$ GPa, $K_0' = 3.5(\pm 0.1)$ with a fixed $V_0 = 162.4$ Å³ for Pv (Fig. 2). The V_0 of Pv25 is much lower than that of Pv, and K_0 is much larger, indicating the potential effect of Fe-spin transitions on the zero-pressure volume and compressibility of perovskite, which will be addressed below. For the well-known tradeoff between K_0 and K_0' , varying the K_0' value by ± 0.5 will cause a 14% change in K_0 and a 1.1% change in V_0 for Pv25. The differential stress in Pv25 has been evaluated using the diffraction peaks 111 and 200 of the Pt pressure standard (Dorfman et al., 2010; Menéndez-Proupin and Singh, 2007; Singh, 1993), indicating that the differential stress is ~ 3 GPa at 130 GPa.

To ascertain the cause for the elevated density and incompressibility in the Fe-rich perovskite, we conducted synchrotron Fe-K β XES and SMS measurements to determine the electronic spin and valence states of iron in the Pv25 samples (e.g. Lin et al., 2005, 2008; Mao et al., 2010). Compared with the reference XES spectra, the XES spectra of Pv25 show a reduction in the intensity of the satellite emission peak (K β') with increasing pressure (Fig. 3). The collected XES spectra of perovskite and reference samples were evaluated using the Integrated Absolute Difference analysis in which the absolute difference between the sample and the reference LS sample was normalized and integrated (Vankó et al., 2006). The total spin momenta (S) of Fe in perovskite were determined by comparing the integral from the sample and the LS reference to that from the HS and LS references. Our analyses showed that the S value slightly decreases from $0.8(\pm 0.2)$ at 80 GPa to $0.6(\pm 0.2)$ at 135 GPa.

The measured SMS spectra were evaluated using the CONUSS program (Sturhahn, 2000). Our analyses showed three distinct Fe sites in perovskite (Fig. 4). Site 1 with 50% abundance exhibits extremely high quadrupole splitting (QS) of $4.10(\pm 0.25)$ mm/s.

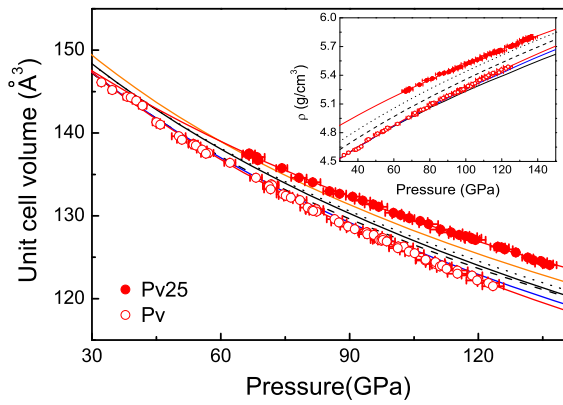


Fig. 2. Pressure-volume relations of perovskite. Red open circles: Pv, this study; red solid circles: Pv25, this study; blue lines: Pv (Fiquet et al., 2000) (with Ar pressure medium and Pt as the pressure calibrant); black solid, dashed, and dotted lines: perovskite with 0, 9 and 15% Fe (with Ar pressure medium and Au as the pressure calibrant), respectively (Lundin et al., 2008); orange line: perovskite with Fe^{3+} (with Ar pressure medium and Au as the pressure calibrant) (Catalli et al., 2010). Corresponding lines represent fits using the third-order Birch–Murnaghan EoS to the experimental results. Uncertainties are smaller than symbols when not shown.

Based on literature hyperfine parameters, this site was assigned to be Fe^{2+} in the dodecahedral sites (e.g. Bengtson et al., 2009; Catalli et al., 2010; Lin et al., 2008; McCammon et al., 2008). However, the spin state of Fe^{2+} with extremely high QS in perovskite is under debate in the literature (Bengtson et al., 2009; Hsu et al., 2010; Lin et al., 2008; McCammon et al., 2008; Narygina et al., 2010). The QS value of site 1 is consistent with recent theoretical predictions that show an extremely high QS for perovskite (Hsu et al., 2010), which was interpreted as a displacement of the HS Fe^{2+} lattice in perovskite (Fig. 5). However, considering the derived S of $0.6 (\pm 0.2)$ from our XES studies, site 1 could also be assigned to be intermediate-spin (IS) Fe^{2+} in the A site (Fig. 5) (Lin et al., 2008; McCammon et al., 2008). Site 2 has a total abundance of 37%, with QS of $2.99 (\pm 0.25)$ mm/s. We assign it to be LS Fe^{3+} in the octahedral sites based on the derived S value from the XES analyses and the obtained hyperfine parameters, together with the QS of Fe^{3+} from the literature (Catalli et al., 2010; Hsu et al., 2011). The QS of site 3 is $1.84 (\pm 0.25)$ mm/s with 13% abundance. This site could be Fe^{3+} either in the HS state or in the LS state (Bengtson et al., 2009; Catalli et al., 2010; Narygina et al., 2010; Xu et al., 2001). According to our SMS and XES analyses, Fe in Pv25 is predominantly Fe^{2+} in the IS state or undergoing an atomic-site change and Fe^{3+} in the LS state.

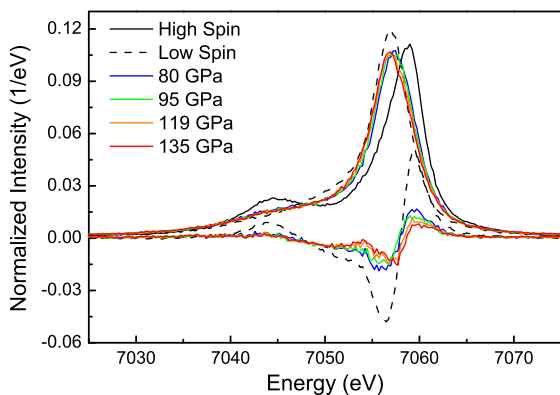


Fig. 3. Fe $K\beta$ X-ray emission spectra of perovskite (Pv25) at high pressures and 300 K. Ferropericlasite with 25% Fe ($(\text{Mg}_{0.75}\text{Fe}_{0.25})\text{O}$, fp25) at ambient conditions is used as the high-spin reference (Mao et al., 2010). fp25 at 90 GPa is used as the low-spin reference (Lin et al., 2010; Mao et al., 2010). The data were analyzed using the Integrated Absolute Difference analysis (Vankó et al., 2006).

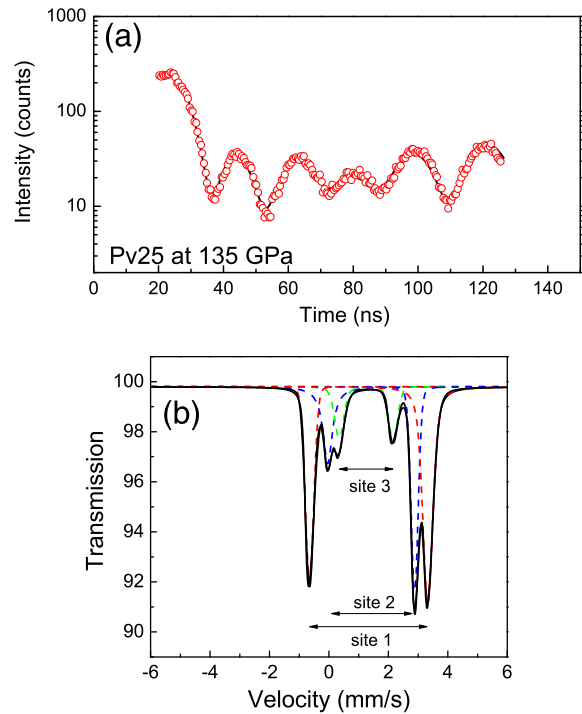


Fig. 4. SMS spectra of Pv25 (a) at 135 GPa and 300 K. (b). Modeled energy spectrum from the evaluation of the measured SMS spectrum.

4. Discussion and conclusion

Using the EoS of Pv25 and Pv from this study and the thermal expansion coefficient and Grüneisen parameter from the literature (Table 1) (Fiquet et al., 2000; Jackson and Rigden, 1996), we have calculated the isothermal bulk modulus, K_T , and bulk sound velocity, V_Φ , as a function of pressure (Fig. 6). For comparison, K_T and V_Φ of Pv25 are respectively 17% and 6% greater than that of Pv at 130 GPa (Fig. 6). Considering experimental uncertainties, previous studies do not show any systematic trend in the EoS of perovskite with increasing Fe content (Fiquet et al., 2000; Lundin et al., 2008) (Fig. 2). Direct comparisons to these studies remain difficult, because they were conducted under variable conditions, using stiffer pressure media and different pressure calibrants (Fiquet et al., 2000; Lundin et al., 2008; McCammon et al., 2008).

Neglecting the role of electronic spin transitions, previous studies on the elasticity of deep-Earth minerals have shown that the addition of iron has a minor effect on their bulk moduli, producing a weak

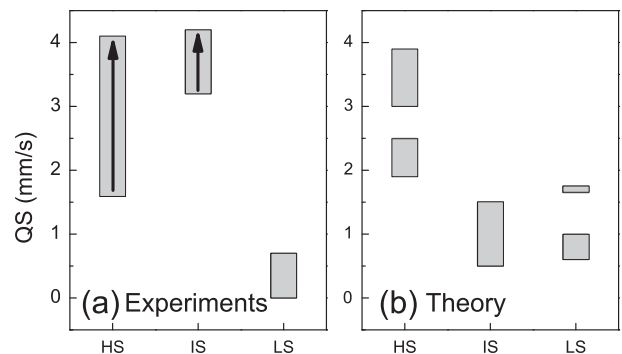


Fig. 5. Quadrupole splitting (QS) of Fe^{2+} in perovskite. (a). experimental results (Grocholski et al., 2009; Jackson et al., 2005; Li et al., 2006; Lin et al., 2008; McCammon et al., 2008, 2010; Narygina et al., 2010); (b). theoretical results (Bengtson et al., 2009; Hsu et al., 2010). Black arrows show the trend of QS with increasing pressure.

Table 1
Thermoelastic parameters of perovskite.

Composition	$\partial K/\partial T$ (GPa/K)	α_0 (10^{-5} K^{-1})	α_1 (10^{-8} K^{-2})	γ^a
Pv ^b	-0.02	2.18	0.11	1.4
Fe-bearing Pv in a peridotite composition ^c	-0.036	3.19	0.88	1.4

^a Jackson and Rigden (1996).

^b Fiquet et al. (2000).

^c Ricolleau et al. (2009).

increase or even a decrease in V_ϕ (Jackson et al., 2006; Jacobsen et al., 2002; Mao et al., 2008; Speziale et al., 2004). For perovskite in particular, the effect of adding Fe on V_ϕ is shown to be weak when the Fe content is less than 15% (Lundin et al., 2008; McCammon et al., 2008), although the presence of 25% Fe can increase the density by 3% at 130 GPa (Fig. 7). The significant increase in the V_ϕ of our Pv25 sample is thus unexpected for mantle minerals and can be understood by the electronic spin transitions of iron in perovskite. Since Fe exists as HS Fe^{2+} and Fe^{3+} in perovskite at relatively low pressures (Bengtson et al., 2009; Catalli et al., 2010; McCammon et al., 2008), this stiffening phenomenon can be explained as a result of the Fe spin transition or atomic-site change in perovskite. We note that the HS to LS transition of Fe^{2+} in ferropericlase has been known to result in an increase in V_ϕ (e.g. Crowhurst et al., 2008; Lin et al., 2005; Wentzcovitch et al., 2009), although a recent experimental study using high-energy resolution inelastic X-ray scattering did not observe a similar increase in V_ϕ of ferropericlase across the spin transition (Antonangeli et al., 2011).

Here, we have modeled the density and V_ϕ of perovskite at relevant lower-mantle pressure and temperature conditions using the thermal Birch–Murnaghan EoS model and our experimental results (Duffy and Anderson, 1989). Considering 75 vol.% of perovskite

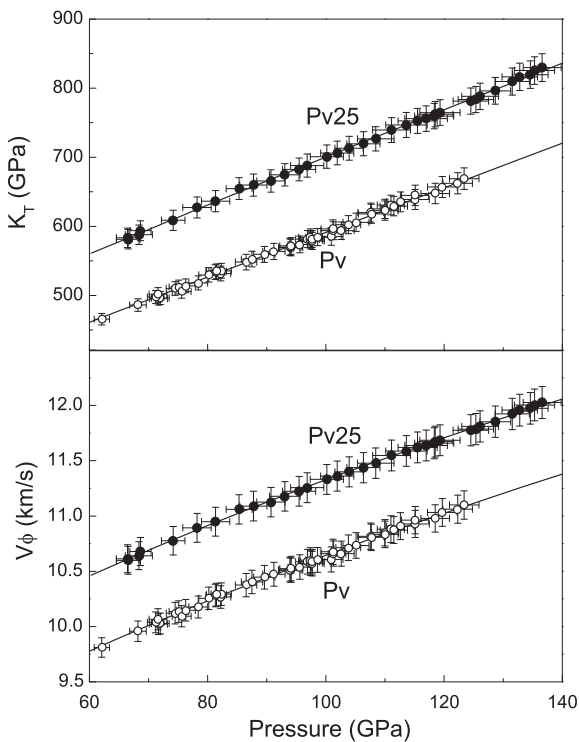


Fig. 6. K_T and V_ϕ of perovskite as a function of pressure at 300 K. Open circles: Pv; solid circles: Pv25. Corresponding lines represent modeled EoS fits to the experimental results. Uncertainties are approximately 2% for K and 1.2% for V_ϕ when fixed $K_0' = 4$ for Pv25. Varying the K_0' value of Pv25 by ± 0.5 can lead to the uncertainty of K and V_ϕ up to 14% and 4%, respectively.

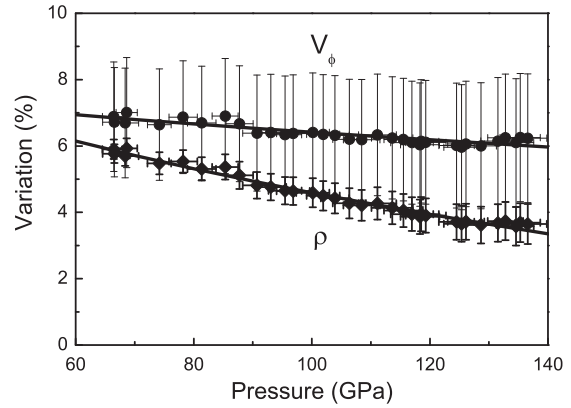


Fig. 7. Density (ρ) and V_ϕ variation of Pv25 using MgSiO_3 perovskite as the reference at lower-mantle pressures. Circles: variation in V_ϕ ; diamonds: variation in ρ . Uncertainties are shown as black bars.

(Hirose, 2002) with an averaged 25% of Fe in the lower mantle along a modeled mantle geotherm, our thermodynamic model shows that lower-mantle perovskite containing 15% excess iron (compared to the average mantle perovskite) would have a density 1–2% and V_ϕ 1.5–3% higher than the surrounding mantle (Fig. 8). The lower mantle is expected to contain 5–10% Al in a pyrolytic composition (e.g. Kesson et al., 1998), although the addition of Al in perovskite is expected to only slightly offset the observed increase in V_ϕ to a lower value and

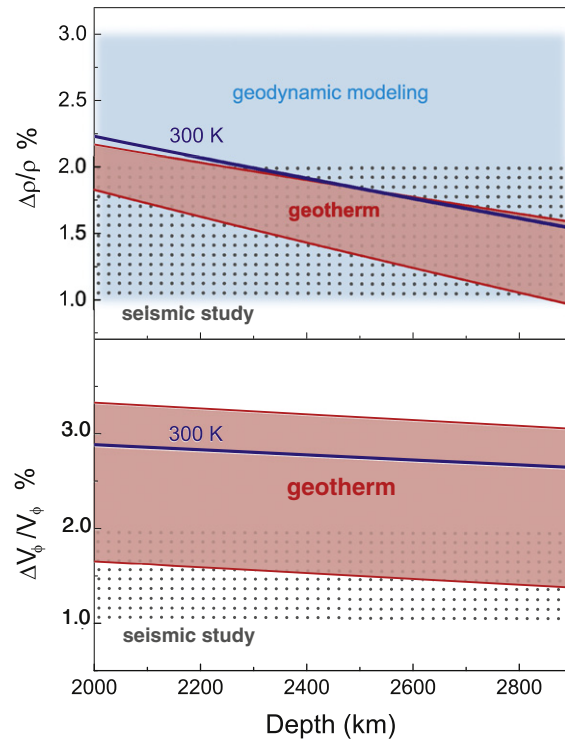


Fig. 8. Modeled ρ and V_ϕ deviation of Pv25 relative to Pv10 along a model mantle geotherm (Brown and Shankland, 1981). $\Delta\rho/\rho$ ($\Delta V_\phi/V_\phi$) represents the density (V_ϕ) difference between Pv25 and Pv10. Blue lines: estimates based on our experimental data at 300 K; red lines and shaded area: calculated deviation along the mantle geotherm (Brown and Shankland, 1981); gray dotted areas: observed maximum seismic anomalies in the LLSVPs (Ishii and Tromp, 1999; Ishii and Tromp, 2004; Su and Dziewonski, 1997; Trampert et al., 2004); blue areas: estimated ρ anomalies in the LLSVPs from thermodynamic modelings (McNamara and Zhong, 2005; Tan and Gurnis, 2005). Uncertainties of the calculated ρ and V_ϕ deviations are plotted as red areas by taking various thermoelastic parameters of perovskite from the literature into account (Fiquet et al., 2000; Ricolleau et al., 2009).

should have a negligible effect on the density (e.g. Yagi et al., 2004). Thus, these increases in density and V_{ϕ} , originating from the electronic spin transitions of iron in perovskite, are consistent with seismic observations of the LLSVPs. Although further investigation as to how electronic spin transitions of iron in perovskite would affect its shear and compressional wave velocities is required, the presence of iron generally results in a decrease in shear-wave velocity (e.g. Jackson et al., 2006; Jacobsen et al., 2002; Mao et al., 2008; Speziale et al., 2004), as is seismically observed in the LLSVPs regions.

The sharply reduced shear-wave velocity and elevated V_{ϕ} and density in the LLSVPs boundaries require a chemical origin such as iron enrichment, but the anti-correlated behavior remains unexplained without considering the effect of spin transitions in lower-mantle minerals (e.g. Hernlund and Houser, 2008; Ishii and Tromp, 2004; Ishii and Tromp, 1999; Su and Dziewonski, 1997; Trampert et al., 2004). Our study provides a potential cause for the LLSVPs, which are suggested to arise not only from thermal anomalies, but also from iron enrichment (Ishii and Tromp, 1999; Trampert et al., 2004). Based on recent geodynamic modeling, LLSVPs may simply represent primordial mantle materials, resulting from core-mantle interactions at the CMB; or be formed by the inclusion of dense, iron-rich material derived from downwelling slabs forming “chemically distinct piles” (Garnero and McNamara, 2008; Knittle and Jeanloz, 1991; McNamara and Zhong, 2005; Tan and Gurnis, 2005). Although Mg-perovskite is increasingly Fe-depleted with depth compared to ferropericlase (e.g. Auzende et al., 2008), the presence of Al is expected to enhance the Fe accommodation in perovskite (Frost and Langenhorst, 2002; McCammon, 1997; Murakami et al., 2004). In this case, Fe-rich perovskite, the potential major phase in the “chemically distinct piles”, would pile up at the bottom of the upwellings because it is too dense to rise. Our studies show that lower-mantle perovskite with approximately 25% iron in the LS Fe^{3+} and IS Fe^{2+} or Fe^{2+} with atomic-site change would satisfy seismic observations for the LLSVPs (Fig. 8) (Hernlund and Houser, 2008; Ishii and Tromp, 2004; Ishii and Tromp, 1999; Trampert et al., 2004). The existence of Fe-rich perovskite piles in the lower mantle would be seismically manifested as velocity and density anomalies in the lower mantle, thus providing a possible explanation for the origin of LLSVPs.

Acknowledgment

We acknowledge C. Jacobs and I. Kantor for experimental assistance. Z. Mao and J. F. Lin acknowledge supports from the US National Science Foundation (EAR-0838221), Energy Frontier Research in Extreme Environments (EFREE), and the Carnegie/DOE Alliance Center (CDAC). Portions of this work were performed at GeoSoilEnviroCARS, Advanced Photon Source, Argonne National Laboratory, supported by the National Science Foundation (EAR-0622171) and Department of Energy (DE-FG02-94ER14466), under Contract No. DE-AC02-06CH11357.

References

- Akahama, Y., Kawamura, H., 2006. Pressure calibration of diamond anvil Raman gauge 20 to 310 GPa. *J. Appl. Phys.* 100, 043516.
- Antonangeli, D., Siebert, J., Aracne, C.M., Farber, D.L., Bosak, A., Hoesch, M., Krisch, M., Ryerson, F.J., Fiquet, G., Badro, J., 2011. Spin crossover in ferropericlase at high pressure: a seismologically transparent transition. *Science* 331, 64–67.
- Auzende, A.-L., Badro, J., Ryerson, F.J., Weber, P.K., Fallon, S.J., Addad, A., Siebert, J., Fiquet, G., 2008. Element partitioning between magnesium silicate perovskite and ferropericlase: new insights into bulk lower-mantle geochemistry. *Earth Planet. Sci. Lett.* 269, 164–174.
- Badro, J., Fiquet, G., Guyot, F., Rueff, J.-P., Struzhkin, V.V., Vankó, G., Monaco, G., 2003. Iron partitioning in Earth's mantle: toward a deep lower mantle discontinuity. *Science* 300, 789–791.
- Badro, J., Rueff, J.-P., Vankó, G., Monaco, G., Fiquet, G., Guyot, F., 2004. Electronic transitions in perovskite: possible nonconvecting layers in the lower mantle. *Science* 305, 383–386.
- Bengtson, A., Li, J., Morgan, D., 2009. Mössbauer modeling to interpret the spin state of iron in (Mg, Fe)SiO₃ perovskite. *Geophys. Res. Lett.* 36, L15301.
- Brown, J.M., Shankland, T.J., 1981. Thermodynamic parameters in the Earth as determined from seismic profiles. *Geophys. J. R. Astron. Soc.* 66, 579–596.
- Catalli, K., Shim, S.-H., Prakapenka, V.B., Zhao, J., Sturhahn, W., Chow, P., Xiao, Y., Liu, H., Cynn, H., Evans, W.J., 2010. Spin state of ferric iron in (Mg, Fe)SiO₃ perovskite and its effect on elastic properties. *Earth Planet. Sci. Lett.* 289, 68–75.
- Crowhurst, J.C., Brown, J.M., Goncharov, A.F., Jacobsen, S.D., 2008. Elasticity of (Mg, Fe)O through the spin transition of iron in the lower mantle. *Science* 319, 451–453.
- Dorfman, S.M., Jiang, F., Mao, Z., Kubo, A., Meng, Y., Prakapenka, V.B., Duffy, T.S., 2010. Phase transitions and equations of state of alkaline earth fluorides CaF₂, SrF₂, and BaF₂ to Mbar pressures. *Phys. Rev. B* 81, 174121.
- Duffy, T.S., Anderson, D.L., 1989. Seismic velocities in mantle minerals and the mineralogy of the upper mantle. *J. Geophys. Res.* 94, 1895–1912.
- Fei, Y., Zhang, L., Corgne, A., Watson, H.C., Ricolleau, A., Meng, Y., Prakapenka, V., 2007a. Spin transition and equations of state of (Mg, Fe)O solid solutions. *Geophys. Res. Lett.* 34, L17307.
- Fei, Y., Ricolleau, A., Frank, M., Mibe, K., Shen, G., Prakapenka, V., 2007b. Towards an internally consistent pressure scale. *Proc. Natl. Acad. Sci. U.S.A.* 104, 9182–9186.
- Fiquet, G., Dewaele, A., Andrault, D., Kunz, M., Bihan, T.L., 2000. Thermoelastic properties and crystal structure of (Mg, Fe)SiO₃ perovskite at lower mantle pressure and temperature conditions. *Geophys. Res. Lett.* 27, 21–24.
- Frost, D.J., Langenhorst, F., 2002. The effect of Al₂O₃ on Fe–Mg partitioning between magnesio-wüstite and magnesium silicate perovskite. *Earth Planet. Sci. Lett.* 199, 227–241.
- Garnero, E.J., McNamara, A.K., 2008. Structure and dynamics of Earth's lower mantle. *Science* 320, 626–628.
- Goncharov, A.E., Struzhkin, V.V., Montova, J.A., Kharlamova, S., Kundargi, R., Siebert, J., Badro, J., Antonangeli, D., Ryerson, F.J., Mao, W., 2010. Effect of composition, structure, and spin state on the thermal conductivity of the Earth's lower mantle. *Phys. Earth Planet. Inter.* 180, 148–153.
- Grocholski, B., Shim, S.-H., Sturhahn, W., Zhao, J., Xiao, Y., Chow, P., 2009. Spin and valence states of iron in (Mg_{0.8}Fe_{0.2})SiO₃ perovskite. *Geophys. Res. Lett.* 36, L24303.
- Hernlund, J.W., Houser, C., 2008. On the statistical distribution of seismic velocities in Earth's deep mantle. *Earth Planet. Sci. Lett.* 265, 423–437.
- Hirose, K., 2002. Phase transitions in pyrolytic mantle around 670-km depth: implications for upwelling of plumes from the lower mantle. *J. Geophys. Res.* 107, 2078.
- Hsu, H., Umamoto, K., Blaha, P., Wentzcovitch, R.M., 2010. Spin states and hyperfine interactions of iron in (Mg, Fe)SiO₃ perovskite under pressure. *Earth Planet. Sci. Lett.* 294, 19–26.
- Hsu, H., Blaha, P., Cococcioni, M., Wentzcovitch, R.M., 2011. Spin-state crossover and hyperfine interactions of ferric iron in MgSiO₃ perovskite. *Phys. Rev. Lett.* 106, 118501.
- Ishii, M., Tromp, J., 2004. Constraining large-scale mantle heterogeneity using mantle and inner-core sensitive normal modes. *Phys. Earth Planet. Inter.* 146, 113–124.
- Ishii, M., Tromp, J., 1999. Normal-mode and free-air gravity constraints on lateral variations in velocity and density of Earth's mantle. *Science* 285, 1231–1236.
- Jackson, I., Rigden, S.M., 1996. Analysis of P–V–T data: constraints on the thermoelastic properties of high-pressure minerals. *Phys. Earth Planet. Inter.* 96, 85–112.
- Jackson, J.M., Sturhahn, W., Shen, G., Zhao, J., Hu, M.Y., Errandonea, D., Bass, J.D., Fei, Y., 2005. A synchrotron Mössbauer spectroscopy study of (Mg, Fe)SiO₃ perovskite up to 120 GPa. *Am. Mineral.* 90, 199–205.
- Jackson, J.M., Sinogeikin, S.V., Jacobsen, S.D., Reichmann, H.J., Mackwell, S.J., Bass, J.D., 2006. Single-crystal elasticity and sound velocities of (Mg_{0.94}Fe_{0.06})O ferropericlase to 20 GPa. *J. Geophys. Res.* 111, B09203.
- Jacobsen, S.D., Reichmann, H.-J., Spetzler, H.A., Mackwell, S.J., Smyth, J.R., Angel, R.J., McCammon, C.A., 2002. Structure and elasticity of single-crystal (Mg,Fe)O and a new method of generating shear waves for gigahertz ultrasonic interferometry. *J. Geophys. Res.* 107, 2741–2744.
- Kesson, S.E., Gerald, J.D.F., Shelley, J.M., 1998. Mineralogy and dynamics of a pyrolytic lower mantle. *Nature* 393, 252–255.
- Kiefer, B., Stixrude, L., Wentzcovitch, R.M., 2002. Elasticity of (Mg, Fe)SiO₃ perovskite at high pressures. *Geophys. Res. Lett.* 29, 1539.
- Knittle, E., Jeanloz, R., 1991. Earth's core-mantle boundary: results of experiments at high pressures and temperatures. *Science* 251, 1438–1443.
- Li, J., Struzhkin, V.V., Mao, H.K., Shu, J., Hemley, R.J., Fei, Y., Mysen, B., Dera, P., Prakapenka, V.B., Shen, G., 2004. Electronic spin state of iron in lower mantle perovskite. *Proc. Natl. Acad. Sci. U. S. A.* 101, 14027–14030.
- Li, J., Sturhahn, W., Jackson, J.M., Struzhkin, V.V., Lin, J.F., Zhao, J., Mao, H.K., Shen, G., 2006. Pressure effect on the electronic structure of iron in (Mg, Fe)(Si, Al)O₃ perovskite: a combined synchrotron Mössbauer and X-ray emission spectroscopy study up to 100 GPa. *Phys. Chem. Minerals* 33, 575–585.
- Lin, J.F., Tsuchiya, T., 2008. Spin transition of iron in the Earth's lower mantle. *Phys. Earth Planet. Inter.* 170, 248–259.
- Lin, J.F., Struzhkin, V.V., Jacobsen, S.D., Hu, M.Y., Chow, P., Kung, J., Liu, H., Mao, H.K., Hemley, R.J., 2005. Spin transition of iron in magnesio-wüstite in the Earth's lower mantle. *Nature* 436, 377–380.
- Lin, J.F., Weir, S.T., Jackson, D.D., Evans, W.J., Vohra, Y.K., Qiu, W., Yoo, C.-S., 2007. Electrical conductivity of the lower-mantle ferropericlase across the electronic spin transition. *Geophys. Res. Lett.* 34, L16305.
- Lin, J.F., Watson, H., Vanko, G., Alp, E.E., Prakapenka, V.B., Dera, P., Struzhkin, V.V., Kubo, A., Zhao, J., McCammon, C., Evans, W.J., 2008. Intermediate-spin ferrous iron in lowermost mantle post-perovskite and perovskite. *Nat. Geosci.* 1, 688–691.
- Lin, J.F., Mao, Z., Jarrige, I., Xiao, Y., Chow, P., Okuchi, T., Hiraoka, N., Jacobsen, S.D., 2010. Resonant X-ray emission study of the lower-mantle ferropericlase at high pressures. *Am. Mineral.* 95, 1125–1131.

- Lundin, S., Catalli, K., Santillan, J., Shim, S.H., Prekopenka, V.B., Junz, M., Meng, Y., 2008. Effect of Fe on the equation of state of mantle silicate perovskite over 1 Mbar. *Phys. Earth Planet. Inter.* 168, 97–102.
- Mao, H.K., Xu, J., Bell, P.M., 1986. Calibration of the ruby pressure gauge to 800 kbar under quasi-hydrostatic conditions. *J. Geophys. Res.* 91, 4673–4676.
- Mao, Z., Jacobsen, S.D., Jiang, F., Smyth, J.R., Holl, C., Frost, D.J., Duffy, T.S., 2008. Single-crystal elasticity of wadsleyites, β - Mg_2SiO_4 , containing 0.37–1.66 wt.% H_2O . *Earth Planet. Sci. Lett.* 268, 540–549.
- Mao, Z., Fu, L.J., Jacobs, C., Watson, H., Xiao, Y., Chow, P., Zhao, J., Alp, E.E., Prakapenka, V.B., 2010. CaIrO_3 -type silicate post-perovskite in the Earth's lowermost mantle. *Geophys. Res. Lett.* 37, L22304.
- Marquardt, H., Speziale, S., Reichmann, H.J., Frost, D.J., Schilling, F.R., E.J., 2009. Elastic shear anisotropy of ferropericlase in Earth's lower mantle. *Science* 324, 224–226.
- McCammon, C., 1997. Perovskite as a possible sink for ferric iron in the lower mantle. *Nature* 387, 694–696.
- McCammon, C., Kantor, I., Narygina, O., Rouquette, J., Ponkratz, U., Sergueev, I., Mezouar, M., Prakapenka, V., Dubrovinsky, L., 2008. Stable intermediate-spin ferrous iron in lower-mantle perovskite. *Nat. Geosci.* 1, 684–687.
- McCammon, C., Dubrovinsky, L., Narygina, O., Kantor, I., Wu, X., Glazyrin, K., 2010. Low-spin Fe^{2+} in silicate perovskite and a possible layer at the base of the lower mantle. *Phys. Earth Planet. Inter.* 180, 215–221.
- McNamara, A.K., Zhong, S., 2005. Thermochemical structures beneath Africa and the Pacific ocean. *Nature* 427, 1136–1139.
- Menéndez-Proupin, E., Singh, A.K., 2007. *Ab initio* calculations of elastic properties of compressed Pt. *Phys. Rev. B* 76, 054117.
- Murakami, M., Hirose, K., Kawamura, K., Sata, N., Ohishi, Y., 2004. Post-perovskite phase transition in MgSiO_3 . *Science* 304, 855–858.
- Narygina, O.V., Kantor, I.Y., McCammon, C.A., Dubrovinsky, L.S., 2010. Electronic state of Fe^{2+} in $(\text{Mg}, \text{Fe})(\text{Si}, \text{Al})\text{O}_3$ perovskite and $(\text{Mg}, \text{Fe})\text{SiO}_3$ majorite at pressures up to 81 GPa and temperatures up to 800 K. *Phys. Chem. Mineral.* 37, 407–415.
- Ohta, K., Onoda, S., Hirose, K., Shinmyo, R., Shimizu, K., Sata, N., Ohishi, Y., Yasuhara, A., 2008. The electrical conductivity of post-perovskite in Earth's D' layer. *Science* 320, 89–91.
- O'Neill, B., Jeanloz, R., 1994. MgSiO_3 – FeSiO_3 – Al_2O_3 in the Earth's lower mantle: perovskite and garnet at 1200 km depth. *J. Geophys. Res.* 99, 19,901–19,915.
- Ricolleau, A., Fei, Y., Cottrell, E., Watson, H.C., Deng, L., Zhang, L., Fiquet, G., Auzende, A.-L., Roskosz, M., Morard, G., Prakapenka, V., 2009. Density profile of perovskite under the lower mantle conditions. *Geophys. Res. Lett.* 36, L06302.
- Singh, A.K., 1993. The lattice strains in a specimen (cubic system) compressed nonhydrostatically in an opposed anvil device. *J. Appl. Phys.* 73, 4278–4286.
- Speziale, S., Duffy, T.S., Angel, R.J., 2004. Single-crystal elasticity of fayalite to 12 GPa. *J. Geophys. Res.* 109, B12202.
- Stackhouse, S., Brodholt, J.P., Price, G.D., 2007. Electronic spin transitions in iron-bearing MgSiO_3 perovskite. *Earth Planet. Sci. Lett.* 253, 282–290.
- Sturhahn, W., 2000. CONUSS and PHOENIX: evaluation of nuclear resonant scattering data. *Hyperfine Interact.* 125, 149–172.
- Su, W.J., Dziewonski, A.M., 1997. Simultaneous inversion for 3-D variations in shear and bulk velocity in the mantle. *Earth Planet. Sci. Lett.* 100, 135–156.
- Tan, E., Gurnis, M., 2005. Metastable superplumes and mantle compressibility. *Geophys. Res. Lett.* 32, L20307.
- Trampert, J., Deschamps, F., Resovsky, J., Yuen, D., 2004. Probabilistic tomography maps chemical heterogeneities throughout the lower mantle. *Science* 306, 853–856.
- Vankó, G., Neisius, T., Molnár, G., Renz, F., Kárpáti, S., Shukla, A., de Groot, F.M.F., 2006. Probing the 3d spin momentum with X-ray emission spectroscopy: the case of molecular-spin transitions. *J. Phys. Chem. B* 110, 11647–11653.
- Wentzcovitch, R.M., Justo, J.F., Wu, Z., Silva, C.R.S., Yuen, D.A., Kohlstedt, D., 2009. Anomalous compressibility of ferropericlase throughout the iron spin cross-over. *Proc. Natl. Acad. Sci. U.S.A.* 106, 8447–8452.
- Xu, W.M., O.N., Rozenberg, G.H., Pasternak, M.P., Taylor, R.D., 2001. Pressure-induced breakdown of a correlated system: the progressive collapse of the Mott–Hubbard state in RFeO_3 . *Phys. Rev. B* 64, 094411.
- Yagi, T., Okabe, K., Nishiyama, N., Kubo, A., Kikegawa, T., 2004. Complicated effects of aluminum on the compressibility of silicate perovskite. *Earth Planet. Sci. Lett.* 143–144, 81–91.
- Zhang, F., Oganov, A.R., 2006. Valence state and spin transitions of iron in Earth's mantle silicates. *Earth Planet. Sci. Lett.* 249, 436–443.